ISSN 1615-9306 · JSSCCJ 41 (22) 4091–4240 (2018) · Vol. 41 · No. 22 · November 2018 · D 10609

JSS

JOURNAL OF

SEPARATION SCIENCE

22|18

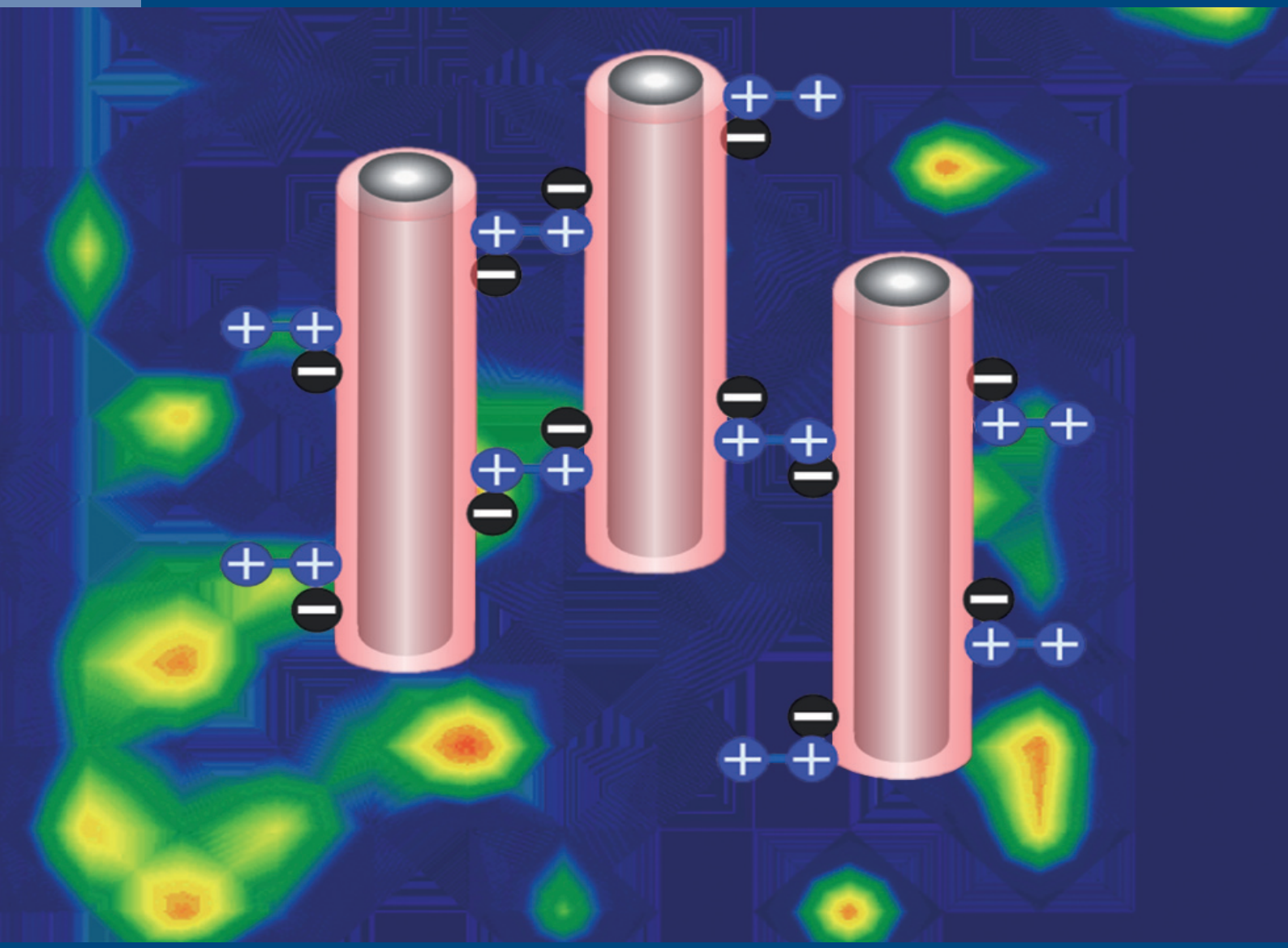

Methods

Chromatography · Electroseparation

Applications

Biomedicine · Foods · Environment

www.jss-journal.com

WILEY-VCH

Received: 28 July 2018 | Revised: 9 September 2018 | Accepted: 14 September 2018

DOI: 10.1002/jssc.201800797

RESEARCH ARTICLE

JOURNAL OF SEPARATION SCIENCE

Preparation of stoichiometric molecularly imprinted polymer coatings on magnetic particles for the selective extraction of auramine O from water

Wenwu Yang[1] | Turghun Muhammad[1] | Aziguli Yigaimu[1] | Kipayem Muhammad[1] | Lingxin Chen[2]

[1]Key Laboratory of Oil and Gas Fine Chemicals, Ministry of Education & Xinjiang Uygur Autonomous Region, College of Chemistry and Chemical Engineering, Xinjiang University, Urumqi, P. R. China

[2]CAS Key Laboratory of Coastal Environment Processes and Ecological Remediation, Chinese Academy of Sciences, Yantai Institute of Coastal Zone Research, Yantai, P. R. China

Correspondence
Dr. Turghun Muhammad, Key Laboratory of Oil and Gas Fine Chemicals, Ministry of Education & Xinjiang Uygur Autonomous Region, College of Chemistry and Chemical Engineering, Xinjiang University, Urumqi 830046, P. R. China.
Email: turghunm@sina.com

A novel magnetic molecularly imprinted polymer for the selective recognition of auramine O was rationally designed via screening from a library of nonimprinted polymers. A stoichiometric ratio of functional monomer (itaconic acid) and template molecule (auramine O) was found to be 1.5. Meanwhile, the synthesized SiO_2@Fe_3O_4 was modified by 0.5 mol/L hydrochloric acid to facilitate the preparation of magnetic molecularly imprinted polymer particles. Adsorption experiments showed that the magnetic polymer particles exhibited good selectivity, recoveries, and enrichment performance. The stoichiometric imprinted polymers have been employed for the selective preconcentration of auramine O from lake water sample. The high specificity of the stoichiometric imprinted polymers was proven in the extraction of mixture solution of auramine O, auramine O hydrochloride, and chrysoidine, and the recoveries ranged between 99.66 and 108.75% (RSD 2.6–3.7%, $n = 3$) for lake water. These results suggest that this method is effective and can be successfully applied to the analysis of auramine O in environmental water samples.

KEYWORDS
auramine O, dispersive solid-phase extraction, dyes, magnetic separation, molecularly imprinted polymers

1 | INTRODUCTION

Nowadays, environmental pollution, food and drug safety have attracted widespread attention all over the world with the improvement of living standard [1,2]. Dyes, as an additive or raw material, play a significant role in our daily life. However, growing concerns have been drawn to the threat of dyes to human health on both toxicological and esthetical aspects [3]. Some industrial dyes, such as Sudan (I–V), pararosaniline, crystal violet, auramine O (AO), and rhodamine B [4–6], are illegally used as additives in a variety of food products to enhance the attractiveness and to compensate limited natural color variation [1,4], and these activities are driven by their low price. In addition, the presence of these dyes in environmental water samples is also becoming an important issue [7–9].

AO is a representative industrial dye and its chemical structure is shown in Supporting Information Figure S1. AO hydrochloride is widely used in the chemical industry for coloring material in paper, textiles, and leather industries [10]. Related research indicated that it could irritate skin, cause conjunctivitis, dermatitis, and upper respiratory irritation symptoms after consumption [5,11]. International Agency for Research on Cancer (IARC) provided sufficient evidence for the carcinogenicity of AO to humans and animals [12]. Considering the potential effects on human health,

Article Related Abbreviations: AO, auramine O; AOHCl, auramine O hydrochloride; DVB, divinylbenzene; IA, itaconic acid; MIP, molecularly imprinted polymer; MMIP, magnetic molecularly imprinted polymer; MNIP, magnetic molecularly non-imprinted polymer; MPS, 3-(trimethoxysilyl)propyl methacrylate; TEOS, tetraethyl orthosilicate

 © 2018 WILEY-VCH Verlag GmbH & Co. KGaA, Weinheim

it is of great importance to develop a sensitive and accurate method for the determination of AO in environmental water samples.

Now, the most widely used analytical methods for the determination of AO are HPLC [5,10] and LC–MS [13,14]. Although these methods are accurate and reliable, they require a number of time-consuming and cumbersome sample preparation steps for complex samples, such as extraction, filteration, and centrifugation. These preparation steps may cause loss and contamination of analyte, as well as consume large amounts of organic solvents. Furthermore, these instruments are relatively expensive and need specialized personnel for the operation and maintenance [15,16]. Therefore, it is of great necessity to develop a simple, economic, green and fast sample pretreatment method for AO.

Molecular imprinting technology has aroused wide concern in researchers all over the world [17–20]. The various molecularly imprinted polymers (MIPs) based on molecular imprinting technology are often considered as ideal host materials for applications including sample pretreatment, chromatography, sensor, and antibody, due to structure predictability, recognition specificity, and application universality [16,17,21,22]. Magnetic molecularly imprinted polymers (MMIPs) could not only overcome some disadvantages of MIPs [23,24], such as incomplete template removal, low binding capacity, slow mass transfer, irregular shape, and heterogeneous distribution of recognition sites, but also exhibit facile separation, higher adsorption performance, and excellent recognition selectivity [25,26].

The ratio of functional monomer and template often plays a vital role in synthesis of molecularly imprinted polymers [17, 27–29], because it can affect the uniform distribution and higher affinity of specific binding sites, as well as the stability and yield of polymers [17,20,28,30]. Herein, a stoichiometric ratio of template and functional monomer is introduced to synthesize MIPs, which further facilitates the advancement and application of imprinted polymer materials [31–33]. It not only overcomes the spatial and steric mismatches of template, but also benefits by forming a highly specific and selective binding site [34,35]. Now, the MIPs of stoichiometric ratio have been widely reported, for example, antibiotics [32], penicillin G [36], s-ibuprofen [34], and tegafur [35]. Thus, a stoichiometric amount of template and monomer is vital for the rational design of a highly specific imprinted material.

In this paper, we report a novel MMIPs based on stoichiometric molecular imprinting. The optimization of polymer composition was carried out based on our previous work [27,30] and other research [33,37,38]. The MMIPs were successfully synthesized using the optimum stoichiometric ratio between template, cross-linker, and functional monomer. It was based on the magnetic Fe_3O_4 particles support, AO as template, itaconic acid (IA) as functional monomer, and divinylbenzene (DVB) as cross-linker. This paper demonstrated a new method of MMIPs preparation and application of the material as the selective adsorption material to analyze water samples from a local lake.

2 | MATERIALS AND METHODS

2.1 | Materials

DVB, tetraethyl orthosilicate (TEOS), azodiisobutyronitrile, and 3-(trimethoxysilyl)propyl methacrylate (MPS) were purchased from J&K Chemical (China). Methanol, acetic acid, acetonitrile, DMSO, and chrysoidine (99%) were obtained from the Sinopharm Chemical Reagent (Shanghai, China). AO hydrochloride (90%, AOHCl) was purchased from Aladdin Chemical Reagent (China). IA was purchased from Sigma Aldrich (China). Ferric chloride ($FeCl_3{\cdot}6H_2O$) was purchased from Tianjin Zhiyuan Chemical Reagent (China). Ferrous sulfate ($FeSO_4{\cdot}7H_2O$) was supplied by Beijing Chemical Factory (China). Ammonium hydroxide ($NH_3{\cdot}H_2O$) was purchased from Xilong Chemical (China). Distilled water was used throughout all experiments.

2.2 | Characterization

Surface morphology was observed by a Hitachi SU 8010 SEM from Hitachi (Honshu, Japan). The morphological evaluation was further visualized by a JEM-2100 TEM from JEOL (Tokyo, Japan). The infrared absorption spectrum was obtained with the KBr method by a Bruker Vertex 70-Equinox 55 FT-IR spectrometer from Bruker (Karlsruhe, Germany). Phase identification was performed by X-Ray powder Diffraction with a Bruker D8 Advance from Bruker (Karlsruhe, Germany). The UV-Vis absorption spectrum was gained with a Shimadzu UV-1800 spectrophotometer from Shimadzu (Kyoto, Japan).

2.3 | Preparation of Fe_3O_4 particles

The process to obtain the Fe_3O_4 particles via chemical coprecipitation method was described previously in the reference [25]. Briefly, 0.01 mol $FeSO_4{\cdot}7H_2O$ and 0.02 mol $FeCl_3{\cdot}6H_2O$ were dissolved completely in 80 mL of deoxygenated distilled water under the nitrogen atmosphere with vigorous mechanical agitation at 800 rpm. The reaction was maintained under nitrogen environment that prevents oxidation. When the solution was preheated to 80°C in water bath, 10 mL of ammonium hydroxide (28, wt%) was added dropwise into the clear yellow solution. With the addition of ammonium hydroxide solution, the mixed solution gradually turned black. After the reaction was maintained at 80°C for 1 h, the magnetic precipitates were separated and isolated by a permanent magnet, and then washed several times with

distilled water. Finally, the obtained black product was dried at 45°C under vacuum for 12 h.

2.4 | Synthesis of SiO_2@Fe_3O_4 particles

The surface modification of the Fe_3O_4 was obtained by the reported method [39]. Briefly, Fe_3O_4 (1.2 g) was dispersed uniformly in 16 mL distilled water and ethanol (80 mL) by sonication for about 5 min. Second, $NH_3{\cdot}H_2O$ (20 mL) and TEOS (8 mL) were added dropwise into the reaction mixture with continuous stirring at 800 rpm under nitrogen atmosphere. The reaction proceeded at room temperature for 12 h under continuous mechanical stirring and nitrogen atmosphere. The product (SiO_2@Fe_3O_4) was collected by magnetic separation with the help of an external permanent magnet, and then was thoroughly washed with deionized water and with dilute hydrochloric acid until neutral, then they were dried at 60°C under vacuum for 12 h.

2.5 | Activation of SiO_2@Fe_3O_4

To improve the silanization of SiO_2@Fe_3O_4, an acid treatment was employed to activate the particles. Fifty milligram of SiO_2@Fe_3O_4 particles were dispersed uniformly in 0.5 mol/L and 1 mol/L hydrochloric acid solutions, and then the mixture was incubated in a shaker at various time conditions of 0.5, 1, 1.5, 2, and 2.5 h, respectively. After that, the activated particles were separated with a magnet and washed with deionized water three times and dried at 60°C for 8 h. Finally, the activated particles were examined using a FTIR spectrometer and the transmittance spectra were analyzed.

2.6 | Synthesis of MPS@SiO_2@Fe_3O_4 particles

The various silanization solvents have been reported to obtain the silanization of SiO_2@Fe_3O_4, however toluene was used most often [40]. In a typical method, SiO_2@Fe_3O_4 (250 mg), anhydrous toluene (50 mL), and MPS (5 mL) were added into a flask successively, and then ultrasonicated for 10 min under nitrogen atmosphere to be dispersed uniformly. After that, the flask was placed in a water bath at 70°C for 12 h with vigorous mechanical stirring (800 rpm) under nitrogen. The products were separated and collected by a permanent magnetic field, and then thoroughly washed with toluene to remove unreacted agents. The final products were dried in a vacuum oven at 60°C for 4 h.

2.7 | Preparation of magnetic polymer particles

MMIP was synthesized by surface imprinting polymerization [25]: the template AO (0.2 mmol) and the functional monomer IA (0.3 mmol) were dissolved in 10 mL DMSO and placed in a 50-mL flask. The mixture was left in contact for several minutes, and then 200 mg of MPS@SiO_2@Fe_3O_4 was dispersed uniformly in the above solution. Subsequently, cross-linker DVB (4.0 mmol) and initiator azodiisobutyronitrile (0.06 mmol) were added into the system and the mixture was degassed in an ultrasonic bath for 5 min. After that, it was purged into nitrogen gas for 10 min to remove oxygen; the polymerization system was carried out at 60°C with nitrogen protection for 24 h. The final product was collected with a help of an external permanent magnet and the particles were washed sequentially with methanol/acetic acid solution (9:1, v:v) [39,41] to remove the entrapped template until there was no template being detected by UV-Vis spectroscopy. The synthesis procedure of AO-imprinted MMIPs was shown in Figure 1. The magnetic molecularly non-imprinted polymers (MNIPs) were synthesized using the same procedure but without template molecule AO.

2.8 | Rebinding experiments

2.8.1 | Batch adsorption experiments

To evaluate the adsorption capacity of the magnetic particles, the adsorption isotherm experiments were conducted with different initial concentrations of AO ranging from 5 to 200 mg/L. The experimental procedures are as follows: 50 mg of particles were equilibrated with 5 mL of a series of AO acetonitrile/water (3:7, v/v) solution in a 10-mL screw cap vials. The mixture was incubated in a shaker at room temperature for 12 h, and then centrifuged and filtrated with 0.45 μm microporous PTFE membrane. Subsequently, the concentration of AO in the supernatant was measured by a UV-Vis spectrophotometer at 436 nm. The equilibrium adsorption capacity (Q, mg/g) was calculated using the following equation:

$$Q = \left(C_0 - C_1\right) \times \frac{V}{m}, \tag{1}$$

where C_0 and C_1 represent the initial solution and final solution concentration (mg/L) of AO, respectively, V is the solution volume (L), and m (g) is the weight of the polymer.

2.8.2 | Selectivity of the magnetic molecularly imprinted polymers

To investigate the specific recognition ability of MMIPs for AO, selectivity tests were carried out using AO, AOHCl, and chrysoidine as structural analogs. Briefly, 50 mg of MMIPs was added into 5 mL, 10 mg/L solution of the above compounds in acetonitrile/water (3:7, v/v), respectively. Then, the mixtures were incubated in a shaker for 12 h at room temperature. The MMIPs were collected by an external magnet and the supernatant was analyzed by UV-Vis spectroscopy after filtration through a 0.45 μm microporous membrane filter. The recognition ability of MMIPs was evaluated by the

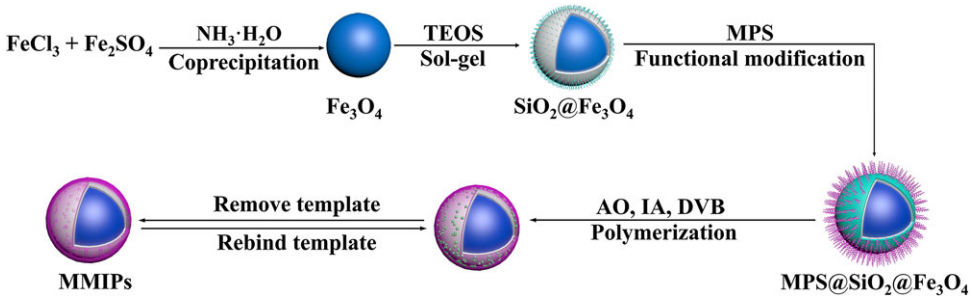

FIGURE 1 Synthesis scheme of MMIPs for auramine O

relative separation factor α(B), which is defined in the following equation:

$$\alpha(B) = \frac{Q_A}{Q_B}, \quad (2)$$

where Q_A and Q_B represent the adsorption amounts of the templates or analogues on MMIPs, respectively.

2.8.3 | Enrichment experiments

To further evaluate the adsorption capacity of MMIPs, 50 mg MMIPs was added into a series of different volume of 2 mg/L AO acetonitrile/water (3:7, v/v) solution. The mixtures were shaken for 12 h at room temperature and the following steps were in common with the batch adsorption experiment. Finally, enrichment performances were evaluated by calculating enrichment factors.

2.9 | Extraction of AO from lake water

The real water samples were sampled from the Red Lake (Xinjiang University, China). The lake water was filtered with a 0.45 μm microporous membrane to remove any possible particulate suspension and mixed with acetonitrile to prepare acetonitrile/water (3:7, v/v) solution, which was stored at 4°C for spiking test. Recovery experiments were carried out using the spiked AO at three concentration levels of 1, 2, and 4 mg/L, and then those samples were analyzed using the UV-Vis spectrophotometer.

3 | RESULTS AND DISCUSSION

3.1 | Preparation of MPS@SiO_2@Fe_3O_4

First, Fe_3O_4 magnetic microspheres were synthesized by the coprecipitation method [25]. Second, the surface of Fe_3O_4 was modified with TEOS through salinization reaction. As shown in Supporting Information Figure S3(a) and (b), SiO_2@Fe_3O_4 particles were activated with hydrochloric acid, which can enhance hydroxyl groups and benefit them by introducing double bonds on the SiO_2@Fe_3O_4 surface. The increase in hydroxyl groups can improve the surface wettability and strengthen the interaction of hydrogen bond [42,43]. In addition, a silica surface is easy to be modified through the covalent reaction [41]. Finally, vinyl groups were introduced onto the surface of activated SiO_2@Fe_3O_4 via MPS coupling, which offered reaction sites for further radical polymerization.

3.2 | Monomer screening

The interaction between template and functional monomer plays an important role in recognition performance of molecularly imprinted polymers [33,38]. Molecular recognition is based on the strength of interactions between the template and the functional monomer, which depends on the shape of cavities in the MIPs [17,20,21]. The screening work of functional monomer and template is based on our previous work [27,30]. In this paper, we choose IA as the functional monomer to synthesize AO imprinted polymer. The carboxyl group of IA can form strong ionic interactions with the basic functional group of AO, and the interaction can enhance the recognition ability [17,26]. Herein, the ratio of functional monomer to template at 1.5 was selected.

3.3 | Characterization of magnetic polymer particles

3.3.1 | SEM and TEM characterization

The morphology of magnetic particles prepared by copolymerization on optimum condition was observed by SEM and TEM. The SEM images of SiO_2@Fe_3O_4, MPS@SiO_2@Fe_3O_4, and MMIPs are shown in Figure 2A–C. It was obvious that a large proportion of all three magnetic particles were in spherical shape and uniform sizes. The size of particles was gradually increasing from SiO_2@Fe_3O_4 to MMIPs. However, the particles aggregate together at some extent after modification for several main reasons: (1) the Fe_3O_4 particles possess strong magnetic interaction that can cause the adhesion and agglomeration; (2) the modification had some influence on the growth of spherical particles during the synthesis; and (3) the polymerization interaction

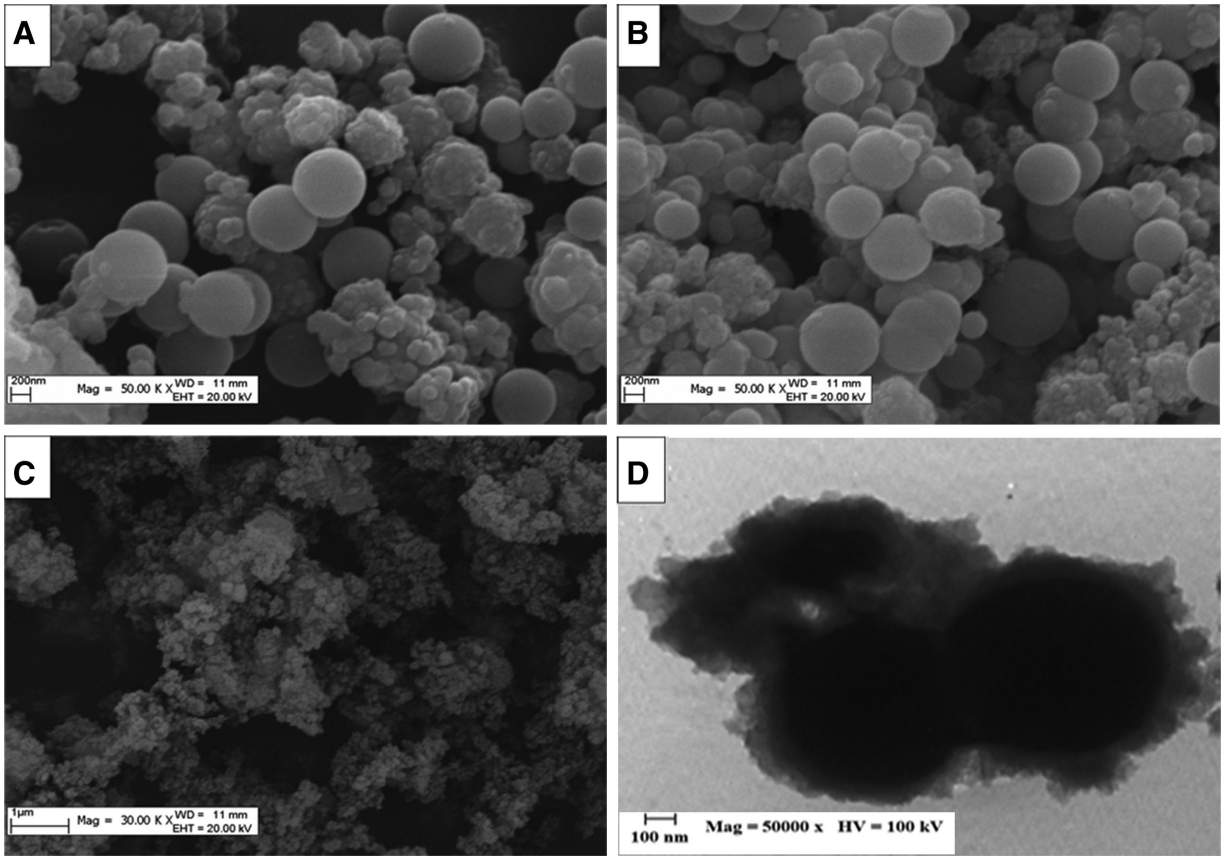

FIGURE 2 The SEM images of (A) SiO_2@Fe_3O_4, (B) MPS@SiO_2@Fe_3O_4, and (C) MMIPs; the TEM image of (D) MMIPs

had great influence on the size of the particle, adhesion, and agglomeration in this study.

Furthermore, the TEM image of MMIPs is shown in Figure 2D. The image of MMIPs showed that the Fe_3O_4 particles as a core (dark), surrounded by a layer (gray) of MMIPs, indicated that MMIPs were coated onto the surface of the Fe_3O_4 particles. However, the surrounding of the core exhibited irregular and lumpy layer that may demonstrate the cavity of template, and the rough surface of MMIPs is beneficial for adsorption of AO.

3.3.2 | FTIR spectroscopy

As shown in Figure 3A, the characteristic peak at 565.47 cm^{-1} corresponds to the stretching vibration of Fe–O. The peak at 1100.48, 945.35, and 800.00 cm^{-1} was attributed to the stretching vibrations of Si–O–Si, Si–O–H, and Si–O, respectively, which indicated that the Fe_3O_4 was successfully modified with TEOS. After activation with 0.5 mol/L hydrochloric acid in Figure 3B, the absorption peak of 3600–3000 cm^{-1} was enhanced, indicating that activation can increase the number of the ─OH groups on the surface of SiO_2@Fe_3O_4, which can promote reaction with the MPS. In Figure 3C, the absorption peaks from 2800 to 3000 cm^{-1} should be attributed to the stretching vibrations of the C–H bond of the $–CH_3$ and $–CH_2$, and the

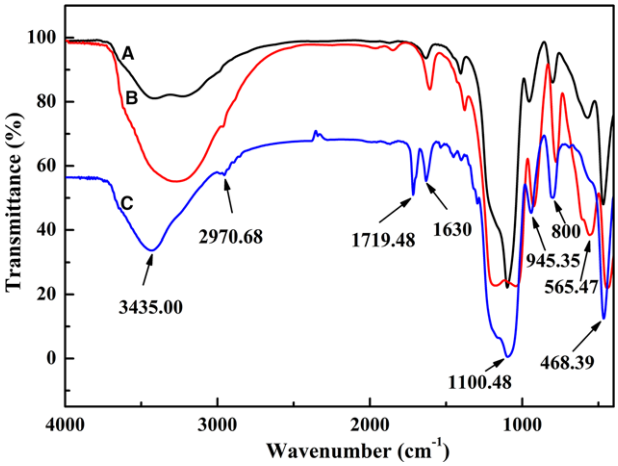

FIGURE 3 The FTIR spectrum of SiO_2@Fe_3O_4 before (A) and after (B) activation, and (C) MPS@SiO_2@Fe_3O_4

peak at 1719.48 cm^{-1} was attributed to the stretching of the –C=O, and those data were the evidence of the successful grafting of MPS. It was observed that the vibration peak at 1630 cm^{-1} corresponding to the stretching vibration of C=C in MPS further proved that SiO_2@Fe_3O_4 was successfully grafted with MPS. Those results are consistent with that of other researches [40,41].

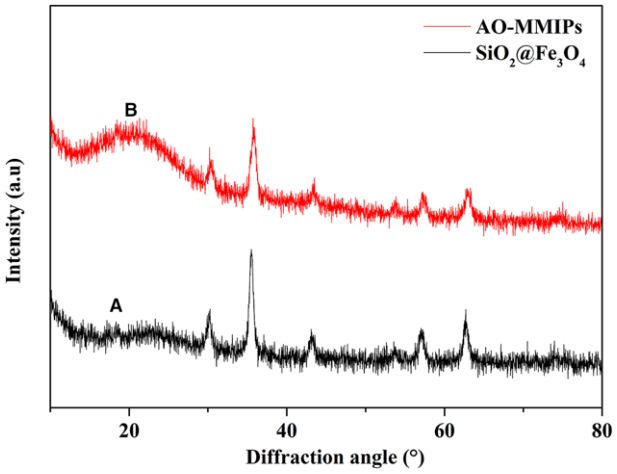

FIGURE 4 XRD patterns of (A) SiO_2@Fe_3O_4 and (B) AO-MMIPs

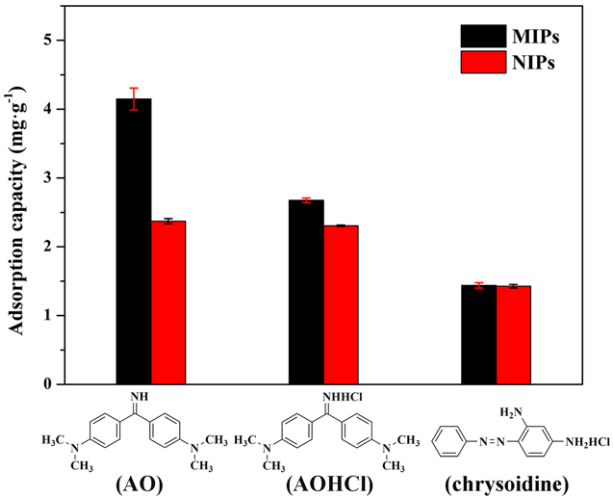

FIGURE 6 Adsorption capacity of MMIPs and MNIPs for AO and its analogues

3.3.3 | XRD analysis

Figure 4 shows the XRD patterns of SiO_2@Fe_3O_4 and AO-MMIPs, and a series of characteristic peaks were observed at 2θ = 30.2, 35.5, 43.1, 53.6, 56.9, and 62.7° for Fe_3O_4 in the 2θ range of 10–80°. These peaks were indexed to the (220), (311), (400), (422), (511), and (440) crystalline planes, respectively, which matched well with the data for magnetite [Joint Committee on Powder Diffraction Standards (JCPDS) card 19-629]. However, a weak signal corresponding to γ-Fe_3O_4 particles were observed and it was almost negligible as compared to Fe_3O_4, because of the oxidation of Fe_3O_4 during the coprecipitation and silanization. The results are almost same to those reported research [44,45].

3.4 | Rebinding and enrichment experiments

The adsorption capacity of MMIPs was investigated by adsorption isotherm experiments. As shown in Figure 5, it

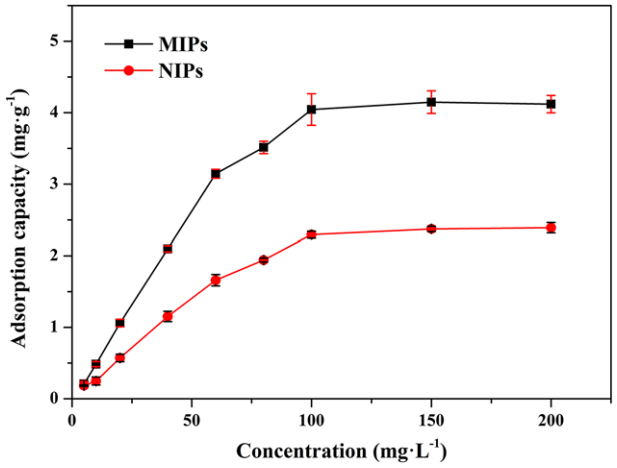

FIGURE 5 Adsorption isotherms of AO on MMIPs and MNIPs

was clearly seen that both MMIPs and MNIPs exhibited good adsorption for AO, and the adsorption capacity of MMIPs continuously increased with the increment of AO ranging from 5 to 100 mg/L and reached equilibrium at 100 mg/L. However, the adsorptive capacity of AO on MMIPs was much higher than that on MNIPs, and the adsorption capacity of MMIPs (4.14 mg/g) was about 1.72-fold over that of MNIPs (2.37 mg/g) at 150 mg/L of AO. The result confirmed that the selectivity of MMIPs was inherently different from that of MNIPs.

The specific recognition ability of MMIPs was evaluated by using AO and its analogues of AOHCl and chrysoidine. Figure 6 illustrates the adsorption capacity of MMIPs and MNIPs for three structurally similar compounds. It can be clearly seen that the adsorption capacity of MMIPs for these compounds is much higher than that of MNIPs. The adsorption capacity of the MMIPs for AO is the highest, which means that template molecule has a higher selective affinity to the MMIPs than its analogues [25]. It may be related to the size and functional groups of recognition sites, and the interaction is mainly due to hydrogen bond and ionic interaction [39,40]. Low adsorption capacity of MMIPs for chrysoidine was observed due to the different structure in comparison with AO and AOHCl, and the adsorption capacity of MNIPs for AO is almost the same with AOHCl, but much higher than chrysoidine due to the structural difference. The relative separation factor was calculated by Formula (2), α(AO/AOHCl) = 1.5 and α(AO/chrysoidine) = 2.9, respectively. In conclusion, the results indicated that the adsorption capacity and selectivity of MMIPs to AO were better than those of other two structural analogues.

As shown in Supporting Information Table S1, the enrichment experiments showed that MMIPs has enrichment capacity to some extent to AO. It can be obviously seen that

TABLE 1 Results of spiked recoveries and RSDs (%; $n = 3$) for determination of AO in real water samples using the MMIPs

Sample	Spiked (mg/L)	Found (mg/L)	Recovery (%)	RSD (%)
1	0	0	–	–
2	1	0.96	96	2.4
3	2	1.99	99.50	3.8
4	4	4.35	108.75	2.6

the binding percentage of MMIPs decrease with the increase in the AO solution volume. However, the enrichment factor appears to be increasing with the solution volume. These results revealed that MMIPs has good enrichment ability. To achieve both high recovery and enrichment, volume of extraction solution was selected to be 5 mL.

3.5 | Application in extraction of AO from lake water

To study the application of MMIPs in practical samples, different concentration of standard solution from 0.5 to 10 mg/L was tested. As shown in Supporting Information Figure S4, a working curve of elution solution absorbance versus initial sampling concentration of AO was established as $y = 0.1473x + 0.0199$, $R^2 = 0.9964$. The determined limits of detection and quantification were 1 and 3.3 mg/L at S/N of 3 and 10, respectively. It is clearly that the working curve has a good linear correlation and the method can be applied for the analysis of the practical samples.

The recovery of the proposed method was further studied using lake water spiked with different concentrations of AO. It was clearly shown in Table 1 that the recoveries were in the range of 95.7–108.8% with RSDs of 2.4–3.8% by the MMIPs. So, the MMIPs were demonstrated to be practically applicable and reliable for sensitive and accurate determination of low AO concentration in real samples.

4 | CONCLUDING REMARKS

In summary, a novel MMIPs based on stoichiometric imprinting was developed and used for the extraction of AO. The MMIPs were synthesized via copolymerization using IA as the functional monomer and DVB as the cross-linker. The analytical method based on MMIPs was successfully employed to analyze the AO of lake water with higher selectivity and enrichment capacity. Herein, this method offers a simple and convenient technique for selective separation and enrichment for AO from complicated water matrices, and also will show great potential applications in convenient preparation of cost-effective, and easy-to-make sample pretreatment materials in the future.

ACKNOWLEDGMENTS

This work was supported by the National Natural Science Foundation of China (21365020 and 21565025) and the 111 Project (D18022).

CONFLICT OF INTEREST

The authors have declared no conflict of interest.

ORCID

Turghun Muhammad http://orcid.org/0000-0001-5562-9365
Lingxin Chen http://orcid.org/0000-0002-3764-3515

REFERENCES

1. Oplatowska-Stachowiak, M., Elliott, C. T., Food colors: existing and emerging food safety concerns. *Crit. Rev. Food. Sci.* 2017, *57*, 524–548.
2. Wang, P. L., Sun, X. H., Su, X. O., Wang, T., Advancements of molecularly imprinted polymers in the food safety field. *Analyst* 2016, *141*, 3540–3553.
3. Xue, X. H., He, X. S., Zhao, Y. H., Adsorptive properties of acid-heat activated rectorite for Rhodamine B removal: equilibrium, kinetic studies. *Desalin. Water Treat.* 2012, *37*, 259–267.
4. Lian, Z. R., Wang, J. T., Determination of crystal violet in seawater and seafood samples through off-line molecularly imprinted SPE followed by HPLC with diode-array detection. *J. Sep. Sci.* 2013, *36*, 980–985.
5. Tatebe, C., Zhong, X. N., Ohtsuki, T., Kubota, H., Sato, K., Akiyama, H., A simple and rapid chromatographic method to determine unauthorized basic colorants (rhodamine B, auramine O, and pararosaniline) in processed foods. *Food Sci. Nutr.* 2014, *2*, 547–556.
6. Zhang, J., Shao, J. B., Guo, P., Huang, Y. M., A simple and fast Fe_3O_4 magnetic nanoparticles-based dispersion solid phase extraction of Sudan dyes from food and water samples coupled with high-performance liquid chromatography. *Anal. Methods* 2013, *5*, 2503–2510.
7. Luo, X. B., Zhan, Y. C., Huang, Y. N., Yang, L. X., Tu, X. M., Luo, S. L., Removal of water-soluble acid dyes from water environment using a novel magnetic molecularly imprinted polymer. *J. Hazard. Mater.* 2011, *187*, 274–282.
8. Ahmad, A., Mohd-Setapar, S. H., Chuong, C. S., Khatoon, A., Wani, W. A., Kumar, R., Rafatullah, M., Recent advances in new generation dye removal technologies: novel search for approaches to reprocess wastewater. *RSC Adv.* 2015, *5*, 30801–30818.

9. Shahid-ul-Islam, S. G., Thermodynamics, kinetics, and multifunctional finishing of textile materials with colorants extracted from natural renewable sources. *ACS Sustain. Chem. Eng.* 2017, *5*, 7451–7466.
10. Li, J. M., Zhai, H. Y., Chen, Z. G., Zhou, Q., Liu, Z. P., Su, Z. H., Preparation and evaluation of a novel molecularly imprinted SPE monolithic capillary column for the determination of auramine O in shrimp. *J. Sep. Sci.* 2013, *36*, 3608–3614.
11. Yan, J. J., Huang, X., Liu, S. P., Yang, J. D., Yuan, Y. S., Duan, R. L., Zhang, H., Hu, X. L., A simple and sensitive method for auramine O detection based on the binding interaction with bovine serum albumin. *Anal. Sci.* 2016, *32*, 819–824.
12. ARC, International Agency for Research on Cancer, ARC, Lyon, France 1987, pp. 118–119.
13. Li, J., Ding, X. M., Liu, D. D., Guo, F., Chen, Y., Zhang, Y. B., Liu, H. M., Simultaneous determination of eight illegal dyes in chili products by liquid chromatography-tandem mass spectrometry. *J. Chromatogr. B* 2013, *942–943*, 46–52.
14. Yin, Y., Ding, T., Liu, H., Zhang, X. Y., Chen, H. L., Determination of chrysoidin, auramine O, astrazon orange G and astrazon orange residue in chillies by solid phase extraction-high performance liquid chromatography-tandem mass spectrometry. *Anal. Lab.* 2014, *33*, 364–368.
15. Wen, Y. Y., Chen, L., Li, J. H., Liu, D. Y., Chen, L. X., Recent advances in solid-phase sorbents for sample preparation prior to chromatographic analysis. *TrAC Trends Anal. Chem.* 2014, *59*, 26–41.
16. Hu, Y. L., Pan, J. L., Zhang, K. G., Lian, H. X., Li, G. K., Novel applications of molecularly-imprinted polymers in sample preparation. *TrAC Trends Anal. Chem.* 2013, *43*, 37–52.
17. Chen, L. X., Wang, X. Y., Lu, W. H., Wu, X. Q., Li, J. H., Molecular imprinting: perspectives and applications. *Chem. Soc. Rev.* 2016, *45*, 2137–2211.
18. Yang, B., Fu, C., Li, J. P., Xu, G. B., Frontiers in highly sensitive molecularly imprinted electrochemical sensors: challenges and strategies. *TrAC Trends Anal. Chem.* 2018, *105*, 52–67.
19. Haupt, K., Mosbach, K., molecularly imprinted polymers and their use in biomimetic sensors. *Chem. Rev.* 2000, *100*, 2495–2504.
20. Bossi, A., Bonini, F., Turner, A. P., Piletsky, S. A., Molecularly imprinted polymers for the recognition of proteins: the state of the art. *Biosens. Bioelectron.* 2007, *22*, 1131–1137.
21. Rutkowska, M., Płotka-Wasylka, J., Morrison, C., Wieczorek, P. P., Namieśnik, J., Marć, M., Application of molecularly imprinted polymers in analytical chiral separations and analysis. *TrAC Trends Anal. Chem.* 2018, *102*, 91–102.
22. Wackerlig, J., Schirhagl, R., Applications of molecularly imprinted polymer nanoparticles and their advances toward industrial use: a review. *Anal. Chem.* 2016, *88*, 250–261.
23. Zhang, J. J., Li, B. Q., Yue, H. J., Zheng, Y. S., Highly selective and efficient imprinted polymers based on carboxyl-functionalized magnetic nanoparticles for the extraction of gallic acid from pomegranate rind. *J. Sep. Sci.* 2018, *41*, 540–547.
24. Gao, R. X., Mu, X. R., Hao, Y., Zhang, L. L., Zhang, J. J., Tang, Y. H., Combination of surface imprinting and immobilized template techniques for preparation of core–shell molecularly imprinted polymers based on directly amino-modified Fe_3O_4 nanoparticles for specific recognition of bovine hemoglobin. *J. Mater. Chem. B* 2014, *2*, 1733–1741.
25. Arabi, M., Ostovan, A., Ghaedi, M., Purkait, M. K., Novel strategy for synthesis of magnetic dummy molecularly imprinted nanoparticles based on functionalized silica as an efficient sorbent for the determination of acrylamide in potato chips: optimization by experimental design methodology. *Talanta* 2016, *154*, 526–532.
26. Yang, W. M., Liu, L. K., Ni, X. N., Zhou, W., Huang, W. H., Liu, H., Xu, W. Z., Computer-aided design and synthesis of magnetic molecularly imprinted polymers with high selectivity for the removal of phenol from water. *J. Sep. Sci.* 2016, *39*, 503–517.
27. Muhammada, T., Liu, C., Wang, J. D., Piletsk, E. V., Guerreiro, A. R., Piletsky, S. A., Rational design and synthesis of water-compatible molecularly imprinted polymers for selective solid phase extraction of amiodarone. *Anal. Chim. Acta* 2012, *709*, 98–104.
28. Hall, A. J., Panagiotis, M., Emgenbroich, M., Quaglia, M., Lorenzi, E. D., Sellergren, B., Urea host monomers for stoichiometric molecular imprinting of oxyanions. *J. Org. Chem.* 2005, *50*, 1732–1736.
29. Gao, R. X., Kong, X., Wang, X., He, X. W., Chen, L. X., Zhang, Y. K., Preparation and characterization of uniformly sized molecularly imprinted polymers functionalized with core–shell magnetic nanoparticles for the recognition and enrichment of protein. *J. Mater. Chem.* 2011, *21*, 17863–17871.
30. Muhammad, T., Nur, Z., Piletska, E. V., Yimit, O., Piletsky, S. A., Rational design of molecularly imprinted polymer: the choice of cross-linker. *Analyst* 2012, *137*, 2623–2628.
31. Wulff, G., Knorr, K., Stoichiometric noncovalent interaction in molecular imprinting. *Bioseparation* 2001, *10*, 257–276.
32. Urraca, J. L., Hall, A. J., MorenoBondi, M. C., Sellergren, B., A stoichiometric molecularly imprinted polymer for the class-selective recognition of antibiotics in aqueous media. *Angew. Chem. Int. Ed.* 2006, *45*, 5158–5161.
33. Terracina, J. J., Bergkvist, M., Sharfstein, S. T., Computational investigation of stoichiometric effects, binding site heterogeneities, and selectivities of molecularly imprinted polymers. *J. Mol. Model.* 2016, *22*, 139–147.
34. Manesiotis, P., Osmani, Q., McLoughlin, P., An enantio-selective chromatographic stationary phase for S-ibuprofen prepared by stoichiometric molecular imprinting. *J. Mater. Chem.* 2012, *22*, 11201–11207.
35. Mattos Dos Santos, P., Hall, A. J., Manesiotis, P., Stoichiometric molecularly imprinted polymers for the recognition of anti-cancer pro-drug tegafur. *J. Chromatogr. B* 2016, *1021*, 197–203.
36. Urraca, J. L., Moreno-Bondi, M. A. C., Hall, A. J., Sellergren, B., Direct extraction of penicillin G and derivatives from aqueous samples using a stoichiometrically imprinted polymer. *Anal. Chem.* 2007, *79*, 695–701.
37. Nicholls, I. A., Andersson, H. S., Charlton, C., Henschel, H., Karlsson, B. C., Karlsson, J. G., O'Mahony, J., Rosengren, A. M., Rosengren, K. J., Wikman, S., Theoretical and computational strategies for rational molecularly imprinted polymer design. *Biosens. Bioelectron.* 2009, *25*, 543–552.
38. Marć, M., Kupka, T., Wieczorek, P. P., Namieśnik, J., Computational modeling of molecularly imprinted polymers as a green

approach to the development of novel analytical sorbents. *TrAC Trends Anal. Chem.* 2018, *98*, 64–78.

39. Chen, F. F., Xie, X. Y., Shi, Y. P., Preparation of magnetic molecularly imprinted polymer for selective recognition of resveratrol in wine. *J. Chromatogr. A* 2013, *1300*, 112–118.
40. Miao, S. S., Wu, M. S., Zuo, H. G., Jiang, C., Jin, S. F., Lu, Y. C., Yang, H., Core-shell magnetic molecularly imprinted polymers as sorbent for sulfonylurea herbicide residues. *J. Agric. Food. Chem.* 2015, *63*, 3634–3645.
41. Wang, D. D., Gao, D., Xu, W. J., Li, F., Yin, M. N., Fu, Q. F., Xia, Z. N., Magnetic molecularly imprinted polymer for the selective extraction of hesperetin from the dried pericarp of Citrus reticulata Blanco. *Talanta* 2018, *184*, 307–315.
42. Zhang, T., Hu, D. Y., Jin, J. H., Yang, S. L., Li, G., Jiang, J. M., Improvement of surface wettability and interfacial adhesion ability of poly(p-phenylene benzobisoxazole) (PBO) fiber by incorporation of 2,5-dihydroxyterephthalic acid (DHTA). *Eur. Polym. J.* 2009, *45*, 302–307.
43. Wang, K. P., Hou, D. Y., Wang, J., Wang, Z. X., Tian, B. H., Liang, P., Hydrophilic surface coating on hydrophobic PTFE membrane for robust anti-oil-fouling membrane distillation. *Appl. Surf. Sci.* 2018, *450*, 57–65.
44. Tang, Y. W., Gao, J. W., Liu, X. Y., Lan, J. X., Gao, X., Ma, Y., Li, M., Li, J. R., Determination of ractopamine in pork using a magnetic molecularly imprinted polymer as adsorbent followed by HPLC. *Food Chem*. 2016, *201*, 72–79.
45. Ashley, J., Wu, K., Hansen, M. F., Schmidt, M. S., Boisen, A., Sun, Y., Quantitative detection of trace level cloxacillin in food samples using magnetic molecularly imprinted polymer extraction and surface-enhanced Raman spectroscopy nanopillars. *Anal. Chem.* 2017, *89*, 11484–11490.

SUPPORTING INFORMATION

Additional supporting information may be found online in the Supporting Information section at the end of the article.

How to cite this article: Yang W, Muhammad T, Yigaimu A, Muhammad K, Chen L. Preparation of stoichiometric molecularly imprinted polymer coatings on magnetic particles for the selective extraction of auramine O from water. *J Sep Sci* 2018;41:4185–4193. https://doi.org/10.1002/jssc.201800797